

Inherent Structures in models for fragile and strong glass

Luca Leuzzi and Theo M. Nieuwenhuizen

Universiteit van Amsterdam

Valckenierstraat 65, 1018 XE Amsterdam, The Netherlands

(printout: October 25, 2018)

An analysis of the dynamics is performed of exactly solvable models for fragile and strong glasses, exploiting the partitioning of the free energy landscape in inherent structures. The results are compared with the exact solution of the dynamics, by employing the formulation of an effective temperature used in literature. Also a new formulation is introduced, based upon general statistical considerations, that performs better. Though the considered models are conceptually simple there is no limit in which the inherent structure approach is exact.

1. INTRODUCTION

The characteristics of a glassy system [1,2] arises from the complex topography of the multidimensional function representing the collective potential energy that gives rise to a non-trivial partition function and thermodynamic potential. In this picture, at low enough temperature where vibrations are minimal, the spatial atomic patterns in crystals and in amorphous systems share the common basic attribute that both represent minima in the potential energy function describing the interactions. The presence of distinct processes acting on two different time-scales means that the deep and wide local minima at and below the glass transition temperature T_g are geometrically organized to create a two scale length potential energy pattern. T_g depends on the cooling procedure and it is usually determined as the temperature at which the viscosity of the glass former reaches the value of 10^{13} Poise.

In the present paper we investigate, using the inherent structure approach, an exactly solvable model glass that shows all the basic features of real glasses [3]. The model is built by processes evolving on two different, well separated time scales, representing respectively the α and β processes taking place in real glassy materials. The slow α processes represents the escape from one deep minimum within a large scale valley to another valley. The fast β processes, instead, are related to elementary relaxations between neighbouring minima inside the same valley. We consider here all kinds of β processes as equivalent, since the characteristic time-scales on which they are evolving are in any case much shorter than the time-scale of the α processes (i.e. the observation time).

In the general case, decreasing the temperature, the free energy local minima can, in principle, be split into smaller local minima. But if we can assume that they maintain their identity in spite of this splitting, we can set a one-to-one correspondence between local minima and inherent structures [4–7], i. e. between the minima of the free energy and the ones of the potential energy. Actually, such a splitting is not even present in the two dynamical models presented here after, making the correspondence clearer.

In this paper we will see to which extent such a scheme, widely used in numerical simulations [4–6,8–12], applies to our analytically solvable model. We will compare it with the exact dynamic solution, achieved without any partitioning of the configuration space.

In section 2 we do introduce the two kinetic models and we give the description of their statics and of their Monte Carlo dynamics. In section 3 we develop the inherent structure approach for the dynamics of such models and we define two different inherent structure effective temperatures mapping the dynamics into a thermodynamic frame (in section 3.3); one definition follows the literature about numerical simulations [4–12], the other exploits the analytic solubility of the models.

2. THE MODELS AND THEIR PROPERTIES

1. Hamiltonian and its constraint

We present two dynamical models, having the same statics, but different dynamics bringing to the behavior of a fragile glass in one instance and to the behavior of a strong glass in the other one. The version describing a system relaxing like a fragile glass was introduced in [13] and widely studied in [3].

Both models are described by the following local Hamiltonian:

$$\mathcal{H}[\{x_i\}, \{S_i\}] = \frac{1}{2}K \sum_{i=1}^N x_i^2 - H \sum_{i=1}^N x_i - J \sum_{i=1}^N x_i S_i - L \sum_{i=1}^N S_i \quad (2.1)$$

where N is the size of the system and $\{x_i\}$ and $\{S_i\}$ are continuous variables, the last satisfying a spherical constraint: $\sum_i S_i^2 = N$. We call them respectively harmonic oscillators and spherical spins. K is the Hooke elastic constant, H is an external field acting on the harmonic oscillators, J is the coupling constant between $\{x_i\}$ and $\{S_i\}$ on the same site i and L is the external field acting on the spherical spins. A separation of time scales is introduced by hand: the spins represent the fast modes and the harmonic oscillators the slow ones. We assume that the $\{S_i\}$ relax to equilibrium on a time scale much shorter than the one of the harmonic oscillators. From the point of view of the motion of the $\{x_i\}$, the spins are just a noise. To describe the long time regime of the $\{x_i\}$, in [3], we did average over this noise by performing the computation of the $\{S_i\}$ partition function, obtaining an effective Hamiltonian depending only on the $\{x_i\}$, that determines the dynamics of these variables. Using the saddle point approximation for large N we got:

$$Z_S(\{x_i\}) = \int \left(\prod_{i=1}^N dS_i \right) \exp \{ -\beta \mathcal{H}[\{x_i\}, \{S_i\}] \} \delta \left(\sum_{i=1}^N S_i^2 - N \right) \quad (2.2)$$

$$\simeq \exp \left[-\beta N \left(\frac{K}{2} m_2 - H m_1 - w + \frac{T}{2} \log \frac{w + \frac{T}{2}}{T} \right) \right]$$

Where we introduced the short-hands

$$m_1 \equiv \frac{1}{N} \sum_{i=1}^N x_i \quad m_2 \equiv \frac{1}{N} \sum_{i=1}^N x_i^2 \quad (2.3)$$

and

$$w \equiv \sqrt{J^2 m_2 + 2JLm_1 + L^2 + \frac{T^2}{4}}. \quad (2.4)$$

We define, then, the effective Hamiltonian $\mathcal{H}_{\text{eff}}(\{x_i\}) \equiv -T \log Z_S(\{x_i\})$, that is the free energy for a given configuration of $\{x_i\}$. We find

$$\mathcal{H}_{\text{eff}}(\{x_i\}) = \frac{K}{2} m_2 N - H m_1 N - w N + \frac{TN}{2} \log \frac{w + \frac{T}{2}}{T} \quad (2.5)$$

This can also be written in terms of the internal energy $U(\{x_i\})$ and of the entropy $S_{\text{ep}}(\{x_i\})$ of the equilibrium processes (i.e. the spins):

$$\mathcal{H}_{\text{eff}}(\{x_i\}) = U(\{x_i\}) - T S_{\text{ep}}(\{x_i\}) \quad (2.6)$$

$$U(\{x_i\}) = \frac{K}{2} m_2 N - H m_1 N - w N + \frac{TN}{2} \quad (2.7)$$

$$S_{\text{ep}}(\{x_i\}) = \frac{N}{2} - \frac{N}{2} \log \frac{w + T/2}{T} \quad (2.8)$$

The function U is actually the Hamiltonian averaged over the spins and S_{ep} is the entropy of the spins.

In [3] we studied the model characterized by a constraint on the phase space, introduced for the fragile glass case to avoid the existence of the single global minimum, and implementing a large degeneracy of the allowable lowest states. The constraint is taken on the $\{x_i\}$, thus concerning the long time regime. It reads:

$$m_2 - m_1^2 \geq m_0 \quad (2.9)$$

where m_0 is a model parameter. It is a fixed but arbitrary, strictly positive constant. This constraint applied to the harmonic oscillators dynamics is a way to reproduce the behavior of good glass formers. We imposed a Monte Carlo dynamics [14,15] satisfying this constraint and coupling the otherwise non-interacting $\{x_i\}$ in a dynamic way. As we saw in [3], the system exhibits a Vogel-Fulcher-Tammann-Hesse (VFTH) relaxation [22], characterizing a fragile glass.

To model a strong glass, instead, we will also consider the same model Hamiltonian but without imposing any constraint and making use of a different Monte Carlo dynamics. We will show later in this paper that this dynamics displays an Arrhenius relaxation near zero temperature. In this case we have a strong glass, as it happens for similar models, e. g. the oscillators model [15] and the spherical spins model [16] where exactly the same dynamics is applied. The new point of the present model is that now both fast and slow processes occur.

To shorten the notation we define the modified ‘‘spring constant’’ \tilde{K} and ‘‘external field’’ \tilde{H} :

$$\tilde{K} = K - \frac{J^2}{w + T/2}, \quad \tilde{H} = H + \frac{JL}{w + T/2} \quad (2.10)$$

We stress that \tilde{K} and \tilde{H} are actually functions of the $\{x_i\}$ themselves (through m_1 and m_2 that occur in w). We also define the constant

$$D \equiv HJ + KL. \quad (2.11)$$

Using the definitions (2.10) it is useful to note that

$$\tilde{H}J + \tilde{K}L = HJ + KL = D. \quad (2.12)$$

2. Statics at heat-bath temperature T

The partition function of the whole system at equilibrium is:

$$\begin{aligned} Z(T) &= \int \mathcal{D}x \mathcal{D}S \exp[-\beta \mathcal{H}(\{x_i\}, \{S_i\})] \delta\left(\sum_i x_i^2 - N\right) = \\ &= \int dm_1 dm_2 \exp\left\{-\beta N \left[\frac{K}{2}m_2 - Hm_1 - w + \frac{T}{2} \log\left(\frac{w + T/2}{T}\right) - \frac{T}{2}(1 + \log(m_2 - m_1^2))\right]\right\} \end{aligned} \quad (2.13)$$

The new object that appears in the exponent is the configurational entropy

$$\mathcal{I} \equiv \frac{N}{2} (1 + \log(m_2 - m_1^2)) \quad (2.14)$$

It comes from the Jacobian $\exp \mathcal{I}$ of the transformation of variables $\mathcal{D}x \rightarrow dm_1 dm_2$, (see (2.3)). We can compute the large N -limit of this partition function using once again the saddle point approximation. The saddle point equations are found minimizing the expression between square brackets in (2.13) with respect to m_1 and m_2 . This yields

$$\bar{m}_1 = \frac{\tilde{H}(\bar{m}_1, \bar{m}_2)}{\tilde{K}(\bar{m}_1, \bar{m}_2)} \quad (2.15)$$

$$\bar{m}_2 = \bar{m}_1^2 + \frac{T}{\tilde{K}(\bar{m}_1, \bar{m}_2)} \quad (2.16)$$

The form of the solutions $\bar{m}_1(T)$, $\bar{m}_2(T)$ is quite complicated because each of these equations is actually a fourth order equation, but they can be explicitly computed. In terms of the equilibrium values \bar{m}_k we find the following expression for the equilibrium free energy:

$$F(T, \bar{m}_1(T), \bar{m}_2(T)) = N \left\{ \frac{K}{2} \bar{m}_2 - H \bar{m}_1 - w(\bar{m}_1, \bar{m}_2) + \frac{T}{2} \left[\log \frac{w(\bar{m}_1, \bar{m}_2) + T/2}{T} - (1 + \log(\bar{m}_2 - \bar{m}_1^2)) \right] \right\} \quad (2.17)$$

$$= U(T, \bar{m}_1, \bar{m}_2) - T S_{\text{ep}}(T, \bar{m}_1, \bar{m}_2) - T \mathcal{I}(T, \bar{m}_1, \bar{m}_2) \quad (2.18)$$

This is the statics both for the model with the constraint (2.9), as long as the temperature exceeds the Kauzmann temperature, and for the one without it. Indeed for the fragile glass case at $T \leq T_0$, when the constraint is reached, the saddle point equation (2.16) becomes $\bar{m}_2 - \bar{m}_1^2 = m_0$, no matter what the temperature of the thermal bath is. In this work, however, we will limit ourselves for the fragile glass to cases where T is slightly larger than T_0 , and for the strong glass case to temperature slightly above zero.

3. Dynamics

The dynamics we apply to the system is a parallel Monte Carlo dynamics firstly introduced in [14]. The thus obtained dynamical model composed by the simple local Hamiltonian (2.1) and such a dynamics has the benefit of being analytically solvable.

In a Monte Carlo step a random updating of the variables is performed ($x_i \rightarrow x'_i = x_i + r_i/\sqrt{N}$) where the $\{r_i\}$ have a Gaussian distribution with zero mean and variance Δ^2 . We define $x \equiv \mathcal{H}(\{x'_i\}) - \mathcal{H}(\{x_i\})$ as the energy difference between the new and the old state. If $x > 0$ the move is accepted with a probability $W(\beta x) \equiv \exp(-\beta x)$; else it is always accepted ($W(\beta x) = 1$). The updating is made in parallel. It is the parallel nature of the updating that allows the collective behavior leading to exponentially divergent time scales in models with no interactions between particles such as ours. A sequential updating would not produce any glassy effect. This dynamics may induce glassy behavior in situations where ordinary Glauber dynamics [17] would not. In our model the parallel dynamics mimics the presence of interactions between atoms in realistic glasses, where a high internal cooperativeness is present. For different examples of dynamics implying non trivial collective behavior the reader can look, for instance, at the n -spin facilitated kinetic Ising model [18,19] or at the kinetic lattice-gas model [20,21].

In a Monte Carlo step the quantities $Nm_1 = \sum_i x_i$ and $Nm_2 = \sum_i x_i^2$ are updated. We denote their change by y_1 and y_2 , respectively. Their distribution function is, for given values of m_1 and m_2 ,

$$\begin{aligned} p(y_1, y_2 | m_1, m_2) &\equiv \int \prod_i \frac{dr_i}{\sqrt{2\pi\Delta^2}} e^{-r_i^2/(2\Delta^2)} \delta\left(\sum_i x'_i - \sum_i x_i - y_1\right) \delta\left(\sum_i x'^2_i - \sum_i x^2_i - y_2\right) \\ &= \frac{1}{4\pi\Delta^2\sqrt{m_2 - m_1^2}} \exp\left(-\frac{y_1^2}{2\Delta^2} - \frac{(y_2 - \Delta^2 - 2y_1m_1)^2}{8\Delta^2(m_2 - m_1^2)}\right) \end{aligned} \quad (2.19)$$

Neglecting the variations of m_1 and m_2 of order Δ^2/N we can express the energy difference as [3]

$$x = \frac{\tilde{K}}{2} y_2 - \tilde{H} y_1, \quad (2.20)$$

In terms of x and $y = y_1$ the distribution function can be formally written as the product of two other Gaussian distributions:

$$\begin{aligned} p(y_1, y_2 | m_1, m_2) dy_1 dy_2 &= dx \frac{p(x | m_1, m_2)}{\sqrt{2\pi\Delta_x}} \frac{dy}{\sqrt{2\pi\Delta_y}} \frac{p(y | x, m_1, m_2)}{\sqrt{2\pi\Delta_y}} \\ &= \frac{dx}{\sqrt{2\pi\Delta_x}} \exp\left(-\frac{(x - \bar{x})^2}{2\Delta_x}\right) \frac{dy}{\sqrt{2\pi\Delta_y}} \exp\left(-\frac{(y - \bar{y}(x))^2}{2\Delta_y}\right) \end{aligned} \quad (2.21)$$

where

$$\bar{x} = \Delta^2 \tilde{K} / 2, \quad \Delta_x = \Delta^2 \tilde{K}^2 (m_2 - m_1^2) + \Delta^2 \tilde{K}^2 \left(m_1 - \tilde{H}/\tilde{K}\right)^2, \quad (2.22)$$

$$\bar{y}(x) = \frac{m_1 - \tilde{H}/\tilde{K}}{m_2 - m_1^2 + \left(m_1 - \tilde{H}/\tilde{K}\right)^2} \frac{x - \bar{x}}{\tilde{K}}, \quad \Delta_y = \frac{\Delta^2 (m_2 - m_1^2)}{m_2 - m_1^2 + \left(m_1 - \tilde{H}/\tilde{K}\right)^2}. \quad (2.23)$$

a. Dynamics of the fragile glass model

To represent a fragile glass the dynamics that we apply to the system is a generalization of the analytic treatment of Monte Carlo dynamics introduced in [14]. As noted in [13], also in this generalized case the dynamical model with a contrived dynamics can be analytically solved. As we saw in [3], in the long-time domain, the dynamics looks quite reasonable with regard to what one might expect of any glassy system and the system exhibits a VFTH relaxation. We repeat here the main steps of the implementation of this dynamics (for a more extended presentation see [3]).

We let Δ^2 , the variance of the random updating $\{r_i\}$, depend on the distance from the constraint, i.e. on the whole $\{x_i\}$ configuration before the Monte Carlo update:

$$\Delta^2(t) \equiv 8[m_2(t) - m_1^2(t)] \left(\frac{B}{m_2(t) - m_1^2(t) - m_0}\right)^\gamma \quad (2.24)$$

where B , m_0 and γ are constants. In particular γ is an exponent larger than zero that appears in the VFTH-like relaxation law of the model, when T decreases towards some critical temperature T_0 (identified in [3] with the Kauzmann temperature):

$$\tau_{\text{eq}} \sim \exp\left(\frac{A_f}{T - T_0}\right)^\gamma \quad (2.25)$$

where A_f is a constant depending on the system's parameters. In other models [14–16,23] the variance Δ^2 was kept constant. The same will also be done for the strong glass version of the model in the next subsection.

For what concerns the exponent γ we saw in [3] that it generates different dynamic regimes for $\gamma > 1$, $\gamma = 1$ and $0 < \gamma < 1$; the situation $\gamma = 1$ remains model dependent even in the long time limit. We will stay in the following in the regime for $\gamma > 1$.

The nearer the system goes to the constraint (i.e. the smaller the value of $m_2 - m_1^2 - m_0$), the larger the variance Δ^2 becomes, implying almost always a refusal of the proposed updating. In this way, in the neighborhood of the constraint, the dynamics is very slow and goes on through very seldom but very large moves, that can be interpreted as activated processes. When the constraint is reached the variance Δ^2 becomes infinite and the system dynamics gets stuck. The system does not evolve anymore towards equilibrium but it is blocked in one single ergodic component of the configuration space. At large enough temperatures, the combination $m_2(t) - m_1^2(t) - m_0$ will remain strictly positive. The highest temperature, T_0 , at which it can vanish for $t \rightarrow \infty$, is identified with the Kauzmann temperature [3].

In [3] the dynamics was expressed in terms of two combinations of m_1 and m_2 . The first one, defined as

$$\mu_1 \equiv \frac{\tilde{H}}{\tilde{K}} - m_1. \quad (2.26)$$

represents the distance from the instantaneous equilibrium state. By instantaneous equilibrium state we mean that \tilde{H} and \tilde{K} depend on the values of m_1 and m_2 at a given time t . For $t \rightarrow \infty$, at the true equilibrium, one has $\mu_1 = 0$.

The second dynamical variable is defined as the distance from the constraint (2.9):

$$\mu_2 \equiv m_2 - m_1^2 - m_0. \quad (2.27)$$

When $\mu_2 = 0$ the constraint is reached. This will happen if the temperature is low enough ($T \leq T_0$) and the time large enough. T_0 is the highest temperature at which the constraint is asymptotically ($t \rightarrow \infty$) reached by the system. Above T_0 ordinary equilibrium will be achieved without reaching the constraint. The temperature is, then, too high for the system to notice that there is a constraint at all on the configurations, and this implies (see (2.16)):

$$\lim_{t \rightarrow \infty} \mu_2(t) = \bar{\mu}_2(T) = \frac{T}{\tilde{K}_\infty(T)} - m_0 > 0, \quad (2.28)$$

where

$$\lim_{t \rightarrow \infty} \tilde{K}(m_1(t), m_2(t); T) \equiv \tilde{K}_\infty(T) = \tilde{K}(\bar{m}_1(T), \bar{m}_2(T)). \quad (2.29)$$

Below T_0 the system goes to configurations that become arbitrarily close to the constraint, and then stay there arbitrarily long. Note that, by definition of T_0 we can write

$$m_0 = \frac{T_0}{\tilde{K}_\infty(T_0)} \quad (2.30)$$

Solving the equations of motions, for fixed parameters (aging setup), we find, to the leading orders of approximation for large times, the following behavior for μ_2 [3]:

$$\mu_2(t) \simeq \frac{B}{[\log(t/t_0) + c \log(\log(t/t_0))]^{1/\gamma}} \quad (2.31)$$

where $c = 1/2$ since in this paper we only look at the regime for $T \geq T_0$. The constant t_0 depends on the parameters of the model and on the temperature; it is of order one. The solution (2.31) is valid in the aging regime, where $t_0 \ll t \ll \tau_{eq}(T)$. Indeed, when $t \sim \tau_{eq}(T) \sim \exp(A/(T - T_0))^\gamma$ the “distance” μ_2 becomes

$$\mu_2 \simeq \frac{B}{\left[\left(\frac{A_f}{T - T_0} \right)^{1/\gamma} \right]^\gamma} \propto T - T_0, \quad (2.32)$$

as it should be.

We also introduce another variable that will be useful later on, namely the difference between $\mu_2(t)$ and its asymptotic, equilibrium, value $\bar{\mu}_2(T)$:

$$\delta\mu_2(t) \equiv \mu_2(t) - \bar{\mu}_2(T) \simeq \frac{B}{[\log(t/t_0) + c \log(\log(t/t_0))]^{1/\gamma}} - \frac{T}{\tilde{K}_\infty(T)} + \frac{T_0}{\tilde{K}_\infty(T_0)} \quad (2.33)$$

where, using (2.30), $\bar{\mu}_2(T)$ comes from (2.28), valid, in the fragile case, when $T \geq T_0$. When $t \rightarrow \infty$ is, by definition, $\delta\mu_2 = 0$.

The dynamical behavior of μ_1 depends not only on the temperature (above or below T_0) but also on γ being greater, equal to or lesser than one. With respect to the relative weight of μ_1 and μ_2 we can identify different regimes, where the solution has different behaviors [3]. What is of our interest here is the regime of $T \geq T_0$ and $\gamma > 1$, where $\mu_1(t) \ll \mu_2(t)$ and a unique effective thermodynamic parameter can be properly defined in various independent ways [3].

b. Dynamics of the strong glass model

We now analyze the simple case without constraint on the configuration space and where Δ^2 , the variance of the randomly chosen updating $\{r_i\}$ of the slow variables $\{x_i\}$, is a constant. This dynamical model can also be seen as the limit for $m_0 \rightarrow 0$ and $\gamma \rightarrow 1$ of the preceding one. We also mention that the case with $J = L = 0$ is the model of harmonic oscillators studied in [15,23].

In the fragile glass case we studied a different version of such a dynamics for two particular combinations of the variables m_1 and m_2 . Here we will keep the same notation. The first variable is thus defined, starting from the saddle point equation (2.15), as the deviation from the instantaneous equilibrium state and is formally equivalent to (2.26).

The second variable is defined as

$$\mu_2 \equiv m_2 - m_1^2. \quad (2.34)$$

When $T = 0$ from equation (2.16) we know that $\mu_2 = 0$. Indeed at $T = 0$ the system reaches its minimum

$$x_i = \frac{H + J}{K} \quad \forall i. \quad (2.35)$$

For simplicity we limit ourselves to a choice of the interaction parameters such that $D = HJ + KL > 0$ and $\tilde{K} > 0$, for which this is the global minimum. In appendix A we derive the equations of motion for μ_1 and μ_2 and we solve them for temperature equal to and slightly above zero and long times, in the aging regime. In this time regime μ_1 comes out to be much smaller than μ_2 : $\mu_1 \propto \mu_2^2$. The solution for μ_2 comes out to be, at the leading order

$$\mu_2(t) \simeq \frac{\Delta^2}{8} \frac{1}{\log \frac{2t}{\sqrt{\pi}}} \quad (2.36)$$

The difference between $\mu_2(t)$ and its asymptotic value is now:

$$\delta\mu_2(t) \equiv \mu_2(t) - \bar{\mu}_2(T) \simeq \frac{\Delta^2}{8} \frac{1}{\log \frac{2t}{\sqrt{\pi}}} - \frac{T}{\tilde{K}_\infty(T)} \quad (2.37)$$

where $\bar{\mu}_2(T)$ comes from (2.16) and

$$\tilde{K}_\infty(T) = \lim_{t \rightarrow \infty} \tilde{K}(m_1(t), m_2(t); T) = \frac{KD}{D + J^2} + \frac{T}{2} \frac{J^2 K^2}{(D + J^2)^2} + \frac{T^2}{8} \frac{J^6 K^3 (J^2 - 3D)}{D(D + J^2)^5} + \mathcal{O}(T^3) \quad (2.38)$$

For $t \rightarrow \infty$, $\delta\mu_2(t) \rightarrow 0$.

At low temperature, the relaxation time for the slow processes depends on the temperature following an Arrhenius law:

$$\tau_{\text{eq}}(T) \propto \exp\left(\frac{A_s}{T}\right); \quad (2.39)$$

$$A_s \equiv \frac{\Delta^2 \tilde{K}_\infty(0)}{8}. \quad (2.40)$$

4. Two temperature thermodynamics

Before going on we recall here that we are able to introduce effective parameters in order to rephrase the dynamics of the system out of equilibrium into a thermodynamic description (for a review see [23]).

In [3] we got through different methods the following expression for the effective temperature in the regime for $T > T_0$ as a function of the interaction parameters of the model and of the time evolution of its observables:

$$T_e(t) = \tilde{K}(m_1(t), m_2(t)) [m_0 + \mu_2(t)] . \quad (2.41)$$

Since we will use one of these methods in the next section to map the IS dynamics into an effective thermodynamic parameter we shortly recall this particular derivation of (2.41). Knowing the solution of the dynamics at a given time t a quasi-static approach can be followed by computing the partition function Z_e of all the macroscopically equivalent states at the time t . In order to generalize the equilibrium thermodynamics we assume an effective temperature T_e and an effective field H_e , and substitute the Boltzmann-Gibbs equilibrium measure by $\exp(-\mathcal{H}_{\text{eff}}(\{x_i\}, T, H_e)/T_e)$, where \mathcal{H}_{eff} is given in (2.6) and the true external field H in it has been substituted by the effective field H_e . As we get the expression of the ‘‘thermodynamic’’ potential $F_e \equiv -T_e \log Z_e$ as a function of macroscopic variables $m_{1,2}$ and effective parameters, we can determine T_e and H_e minimizing F_e with respect to m_1 and m_2 and evaluating the resulting analytic expressions at $m_{1,2} = m_{1,2}(t)$.

The partition function of the macroscopically equivalent states is:

$$Z_e(m_1, m_2; T_e, H_e) \equiv \int \mathcal{D}x \exp \left[-\frac{1}{T_e} \mathcal{H}_{\text{eff}}(\{x_i\}, T, H_e) \right] \delta(Nm_1 - \sum_i x_i) \delta(Nm_2 - \sum_i x_i^2), \quad (2.42)$$

From this we build the effective thermodynamic potential as a function of T_e and H_e , besides of T and H , where the effective parameters depend on time through the time dependent values of m_1 and m_2 , solutions of the dynamics. They are actually a way of describing the evolution in time of the system out of equilibrium. The free energy $F_e = -T_e \log Z_e$ is minimized with respect to m_1 and m_2 . Then their time dependent values are inserted, yielding

$$F_e(t) = U(m_1(t), m_2(t)) - TS_{ep}(m_1(t), m_2(t)) - T_e(t)\mathcal{I}(m_1(t), m_2(t)) + [H - H_e(t)]Nm_1(t), \quad (2.43)$$

with

$$\begin{aligned} T_e(t) &= \tilde{K}(m_1(t), m_2(t)) [m_0 + \mu_2(t)], \\ H_e(t) &= H - \tilde{K}(m_1(t), m_2(t)) \mu_1(t). \end{aligned} \quad (2.44)$$

where T_e is the so called effective temperature. U is the internal energy of the whole system, S_{ep} is the entropy of the fast or equilibrium processes (the spherical spins) while \mathcal{I} is the entropy of the slow, ‘‘configurational’’, processes (the harmonic oscillators). The last term of F_e replaces the $-HNm_1$ occurring in U (see eq. (2.7)) by $-H_eNm_1$. U , S_{ep} and \mathcal{I} are ‘state’ functions, in the sense that they depend on the state described by T , T_e , H and, if needed, H_e . In the framework where only one relevant effective parameter T_e stays, these functions do not depend on the path along which its value has been reached.

As we saw in [3] for the VFTH relaxing model at $T > T_0$ and in appendix A for the Arrhenius relaxing case (A.25), (A.35), the effective temperature alone is enough for a complete thermodynamic description of the dominant physical phenomena ($H_e = H$). The introduction of H_e becomes important only for second order corrections in $\delta\mu_2$.

3. INHERENT STRUCTURE APPROACH

The characteristics of a glassy system can be represented by means of a multidimensional potential energy function with a complex topography. The spatial patterns of atoms in crystals and in amorphous systems, at low temperature, represent, then, minima in the potential energy function describing the interactions [4,5].

In the case of the model (2.1) all the complex chemical properties of real glass formers are not present, but nevertheless the system exhibits several aspects of their complex features (described in [3]), indicating that our simple model is complicated enough for what concerns the description and the comprehension of the basic long time properties of a glass.

In a real glass the presence of distinct processes (acting on different time-scales) can be obtained from a careful analysis of the relaxation response function above T_g . We limit ourselves to a two time-scale approach. This means that the deep and wide local minima at and below T_g are geometrically organized to create a two scale length potential

energy pattern. As a consequence the system shows α and β processes. The α processes represents the escape from one deep minimum within a large scale valley to another valley. This escape requires a lengthy directed sequence of elementary transitions producing a very large activation energy. Moreover, the high lying minima between any two valleys, among which the system is making a transition, are very degenerate. This implies a large activation entropy for the *inter-basin* transition. β processes are instead related to elementary relaxations between neighboring minima (*intra-basin* dynamics).

We stress that in our models we put together all kind of β processes in our short time-scale, since they are in any case much shorter than the observation time considered.

1. Decomposition of the partition function: introduction of inherent structures

In this point of view an approximate approach to the problem is to divide the complicated multidimensional landscape of the (potential) energy in structures formed by large deep basins and to describe the dynamics of the processes taking places as intra-basin and inter-basin [4,5].

More precisely one can define an *Inherent Structure* (IS) as that basin behind an actual configuration of the system evolving in time at some temperature T that is the minimum of the potential energy reached in an instantaneous quenching by the method of *steepest descent*.

The introduction of IS's allows, at low enough temperature ($T < T_g$), a decomposition of the partition function into an IS part, connected to the zero temperature landscape corresponding to the configurations of the system at temperature T , and a part connected to the thermal excitation of the configurations in a single minimum.

The probability that an equilibrium configuration at $T = 1/\beta$ belongs to a basin associated with an IS structure with an energy density in the interval $[e, e + de]$ is [4,9–11]

$$\mathcal{P}(e, T)de \propto \exp(-\beta N [e - Ts_c(e) + f_v(e, T)]) de \quad (3.1)$$

where $s_c(e)$ is proportional to the logarithm of the number of IS's existing at the energy level e and $f_v(e, T)$ is the free energy of the configurations inside an IS at energy e (related to a temperature T system). To derive the distribution (3.1) in this form the approximation is made that f_v is computed as the average over all the IS's of energy e . This means that, by assumption, the shape of a basin depends only on its energy level and on the temperature. Enough below T_g the further approximation can be made, that $f_v(e, T) \sim f_v(T)$, because fluctuations inside one IS are small [8,9]. The shape of the basin depends then only on the temperature. All the internal (vibrational) states of any IS have the same (vibrational) free energy f_v at given T . We anticipate, however, that in the present study we will not carry out such an approximation for our models.

IS dynamics is significant, i.e. significantly represents the actual dynamics of the system at finite T , provided that there is a one to one correspondence between IS's and real minima at finite temperature and provided that these IS's are visited with the same frequency with which the corresponding finite T minima are visited.

2. Inherent Structure approach in the Harmonic Oscillator-Spherical Spin model

As we will see, the model (2.1) is built in such a way that every $\{x_i\}$ configuration is an inherent structure. Indeed, at a given $\{x_i\}$ configuration at finite T , the $\{S_i\}$ are fast variables and they contribute to the energy and to the other observables as a noise depending on temperature. If we take away this contribution we do not actually change the configurations of the minima of the slow variables. In the case of the system without constraint on the configuration space, nor contrived dynamics, any $\{x_i\}$ configuration is an inherent structure. For what concerns the constrained model, instead, certain configurations are not allowed. Moreover the presence of the constraint (2.9) produces (entropic) barriers higher than in the other case to get from a certain IS to a different one. That just means that the dynamics through the inherent structures is even slower in the fragile glass case than in the strong glass case.

First of all we have to define the steepest descent procedure for the model. We start performing the minimization of

$$\mathcal{H} + \lambda \sum_{i=1}^N S_i^2 - \lambda N, \quad (3.2)$$

where \mathcal{H} is the Hamiltonian (2.1) of the model and where we implemented the spherical constraint $\sum_i S_i^2 = N$ by using the Lagrange multiplier λ .

To get rid of the contribution of the spins, i.e. to get rid of the fast modes, we minimize (3.2) with respect to the $\{S_i\}$. We get

$$S_i^{(\min)} = \frac{\beta(Jx_i + L)}{2\lambda} \quad \forall i \quad (3.3)$$

Inserting this values for S_i and solving for λ we, then, find

$$\lambda = \frac{\beta}{2} w_{\text{is}} \quad (3.4)$$

where m_1 and m_2 are defined in (2.3) and

$$w_{\text{is}} \equiv \sqrt{J^2 m_2 + 2JLm_1 + L^2}. \quad (3.5)$$

Using (3.4) the minimum $\{S_i\}$ configuration for a given set of $\{x_i\}$ is, thus, given by

$$S_i^{(\min)} = \frac{Jx_i + L}{w_{\text{is}}} \quad \forall i. \quad (3.6)$$

Finally the expression (3.2) becomes

$$\mathcal{H}_{\text{is}} \equiv N \left[\frac{K}{2} m_2 - H m_1 - w_{\text{is}} \right] \quad (3.7)$$

that is the energy function of the inherent structures. Consequently the partition sum over inherent structures is defined by

$$Z_{\text{is}} = \int \mathcal{D}x \exp[-\beta \mathcal{H}_{\text{is}}] = \int dm_1 dm_2 \exp(\mathcal{I} - \beta \mathcal{H}_{\text{is}}) \quad (3.8)$$

Due to the minimization any explicit dependence on T disappears with respect to the effective Hamiltonian (2.5). In (2.2), integrating over the spins, instead of minimizing with respect to them, we also had an entropic term for the fast processes (S_{ep} given in (2.8)) and a slightly different internal energy (Nw instead of Nw_{is}). Carrying out steepest descent the entropic term vanishes (only the minimal configuration is taken into account) and the inherent structure energy has no explicit dependence on the temperature. The configurational entropy for IS's comes from the Jacobian of the transformation of variables $\mathcal{D}x = e^{\mathcal{I}} dm_1 dm_2$, (see (2.3) and (2.14)). It is the same of the finite T case, since any allowed configuration $\{x_i\}$ is also an IS.

The static average of \mathcal{H}_{is} is given by

$$E_{\text{eq}}^{\text{is}}(T) = \mathcal{H}_{\text{is}}(\overline{m}_{1,2}^{\text{(is)}}(T)) \quad (3.9)$$

where $\overline{m}_{1,2}^{\text{(is)}}(T)$ are the solutions of the saddle point equations that we get in the IS case to compute (3.8), in the limit of large N . The equations are

$$\overline{m}_1^{\text{(is)}} = \frac{D}{J(K - J^2/w_{\text{is}})} - \frac{L}{J} = \frac{\tilde{H}_{\text{is}}}{\tilde{K}_{\text{is}}} \quad (3.10)$$

$$\overline{m}_2^{\text{(is)}} - (\overline{m}_1^{\text{(is)}})^2 = \frac{T}{D}(J\overline{m}_1^{\text{(is)}} + L) = \frac{T}{\tilde{K}_{\text{is}}} \quad (3.11)$$

where we define

$$\tilde{H}_{\text{is}} \equiv H + \frac{JL}{w_{\text{is}}} \quad ; \quad \tilde{K}_{\text{is}} \equiv K - \frac{J^2}{w_{\text{is}}} \quad (3.12)$$

with w_{is} from (3.5). The combination $\tilde{H}_{\text{is}}J + \tilde{K}_{\text{is}}L = HJ + KL = D$ is, again, simple, as in (2.12).

In the case at finite T the static partition function (2.13) was

$$Z = \int dm_1 dm_2 \exp(\mathcal{I} - \beta \mathcal{H}_{\text{eff}}), \quad (3.13)$$

with \mathcal{H}_{eff} defined in (2.5) and \mathcal{I} in (2.14). The two saddle point equations are different from (2.15) and (2.16) valid in the realistic case, giving thus different results: $\overline{m}_{1,2}^{(\text{is})} \neq \overline{m}_{1,2}$. We note explicitly that $\overline{m}_{1,2}^{(\text{is})}$ depends on T even in the IS case.

Comparing the expressions so far obtained with those appearing in the exponent of the probability distribution (3.1) we identify the configurational entropy Ns_c with \mathcal{I} , as defined in (2.14), and the rest with

$$N(e + f_v) = \mathcal{H}_{\text{eff}}(\{x_i\}) = \mathcal{H}_{\text{is}}(\{x_i\}) + F_v(\{x_i\}) \quad (3.14)$$

where, as already told, $\mathcal{H}_{\text{is}}(\{x_i\})$ is the IS internal energy and from the difference $\mathcal{H}_{\text{eff}}(\{x_i\}) - \mathcal{H}_{\text{is}}(\{x_i\}) = F_v(\{x_i\})$ the thermal free energy of one IS turns out to be:

$$F_v = \frac{T}{2} \log \left(\frac{w + T/2}{T} \right) - N(w - w_{\text{is}}) . \quad (3.15)$$

where w is defined in (2.4) and w_{is} in (3.5). Notice that it explicitly depends on the parameters m_1 and m_2 of the IS, whereas in literature it is often assumed to be a constant (harmonic approximation [4,5,8–11]).

3. Effective temperature in the IS's approach

a. Expansion of the dynamical energy

A possible way of defining an effective temperature, sometimes used in literature, for instance in the study of Lennard-Jones interacting spheres [8,9] and in the study of the random orthogonal model [10], is to compare the time dependent out of equilibrium mean internal energy with the equilibrium mean internal energy expression at a temperature $T_e \neq T$. The out of equilibrium mean internal energy is built taking the dynamics of a system out of equilibrium at temperature T and repeating it many times starting from different initial conditions. A statistical ensemble of trajectories is constructed in this way. At any given time t the configurations that each sample is visiting are found. The energy \mathcal{H}_{is} averaged over the ensemble of different trajectories is,

$$E_d^{(\text{is})}(t) \equiv \langle \mathcal{H}_{\text{is}} \rangle_t \equiv N \frac{K}{2} m_2(t) - NHm_1(t) - N \sqrt{J^2 m_2(t) + 2JLm_1(t) + L^2} \quad (3.16)$$

$$\simeq N \frac{K}{2} \overline{m}_2^{(\text{is})} - NH \overline{m}_1^{(\text{is})} - N \sqrt{J^2 \overline{m}_2^{(\text{is})} + 2JL \overline{m}_1^{(\text{is})} + L^2} + N \tilde{K}_{\text{is}}(\overline{m}_1^{(\text{is})}, \overline{m}_2^{(\text{is})}) \delta \mu_2(t) + C(\overline{m}_1^{(\text{is})}, \overline{m}_2^{(\text{is})}) \delta \mu_2(t)^2 \quad (3.17)$$

$$\simeq E_{\text{eq}}^{(\text{is})}(T) + N \tilde{K}_{\text{is}}(\overline{m}_1^{(\text{is})}, \overline{m}_2^{(\text{is})}) \delta \mu_2(t) + C(\overline{m}_1^{(\text{is})}, \overline{m}_2^{(\text{is})}) \delta \mu_2(t)^2 \quad (3.18)$$

where $\delta \mu_2(t) \equiv \mu_2(t) - \overline{\mu}_2(T)$ is given by (2.37) in the Arrhenius case and by (2.33) in the constrained case for $T \geq T_0$. The equilibrium IS energy $E_{\text{eq}}^{(\text{is})}(T)$ will be a different function of the temperature in the two dynamic versions of the model. The second order expansion will be needed only for the strong glass case and the expression for the factor $C(\overline{m}_1^{(\text{is})}, \overline{m}_2^{(\text{is})})$ is, in that case:

$$C(\overline{m}_1^{(\text{is})}, \overline{m}_2^{(\text{is})}) = \frac{DJ^4 K^2}{8(D + J^2)^4} . \quad (3.19)$$

We can then take a system in equilibrium at a temperature T_e , such that the configurations visited by the system at equilibrium are the same as those out of equilibrium at temperature T . This we call effective temperature. In other words, fixing t , T_e is defined as the temperature at which the system at equilibrium would visit the same configurations visited by the system out of equilibrium at temperature T , with the same frequency.

b. The effective temperature employed in numerical approaches: the fragile case

Following the approach found in literature [8–10] for numerical simulations, we can define a $T_{e1}^{(\text{is})}$ through the matching of the equilibrium and the out of equilibrium IS internal energy: it is the one such that

$$E_{\text{eq}}^{(\text{is})}(T_{e1}^{(\text{is})}(t)) = E_d^{(\text{is})}(t) \quad (3.20)$$

For our model it is possible to work out an analytic expression for such a $T_{e1}^{(\text{is})}(t)$, at least near the Kauzmann transition for the fragile glass case, linearizing in $T - T_0$.

What we get is a parameter different from the thermodynamic effective temperature (2.41) that we got from three different approaches (including the Fluctuation-Dissipation Ratio) in [3].

For the fragile glass case we are not able to derive any simple expression, of the IS energy (3.16), but we can in any case solve it exactly. The results are shown in figures 3.1-3.2 for a given choice of the values of the interaction parameters of the model. As one can see $T_{e1}^{(\text{is})}(t)$ comes out to be different from $T_e(t)$ at any time decade.

As a matter of fact what we are comparing now with the average $E_d(t)$ is a function $E_{eq}(T_{e1}^{(\text{is})})$ of the effective temperature alone, while we know that out of equilibrium any proper thermodynamic function cannot simply depend on just one temperature as the thermodynamic function of equilibrium systems do [23]. It is not surprising, thus, that the two functions do not coincide.

c. The effective temperature employed in numerical approaches: the strong case

For the strong glass case it is possible to work out a simple analytic expression for the dynamical and the equilibrium IS energy. To do it we will expand near zero temperature up to second order in T .

We underline that the thermodynamic effective temperature given in (2.41) is also the expression of the effective temperature for the system without constraint. What changes in that case is the time behavior of $m_2 - m_1^2 = \mu_2$, that is now given by (2.36), and its limit at equilibrium (see (2.16)). In this case, where the analytic treatment is by far easier, we can give a short explicit expression for $T_{e1}^{(\text{is})}(t)$:

$$T_{e1}^{(\text{is})} \simeq T + \frac{KD}{D+J^2}\delta\mu_2(t) + \frac{J^4K^2}{2(D+J^2)^3}T\delta\mu_2(t) + \mathcal{O}(T^3) + \mathcal{O}(\delta\mu_2(t)^3) . \quad (3.21)$$

Here above terms of $\mathcal{O}(T^2)$ and $\mathcal{O}(\delta\mu_2(t)^2)$ cancel. This $T_{e1}^{(\text{is})}(t, T)$ is obtained from (3.20) with

$$\begin{aligned} \frac{E_d^{(\text{is})}(t)}{N} \simeq & -\frac{(H+J)^2}{2K} - L + \frac{T}{2} - \frac{J^4K}{8D(D+J^2)^2}T^2 + \frac{KD}{2(D+J^2)}\delta\mu_2(t) + \frac{J^4K^2}{8D(D+J^2)^2}T\delta\mu_2(t) + \frac{DJ^4K^3}{8(D+J^2)^4}\delta\mu_2(t)^2 \\ & + \mathcal{O}(T^3) + \mathcal{O}(T^2\delta\mu_2(t)) + \mathcal{O}(T\delta\mu_2(t)^2) + \mathcal{O}(\delta\mu_2(t)^3) \end{aligned} \quad (3.22)$$

If we expand (2.41) in the same way we get:

$$\begin{aligned} T_e = T + \tilde{K}\delta\mu_2(t) = & T + \frac{KD}{D+J^2}\delta\mu_2(t) + \frac{T}{2} \left(\frac{JK}{D+J^2} \right)^2 \delta\mu_2(t) + \frac{DJ^4K^3}{2(D+J^2)^4}\delta\mu_2(t)^2 \\ & + \mathcal{O}(T^3) + \mathcal{O}(T^2\delta\mu_2(t)) + \mathcal{O}(T\delta\mu_2(t)^2) + \mathcal{O}(\delta\mu_2(t)^3) \end{aligned} \quad (3.23)$$

As we see from the formulae above and from figures 3.3 and 3.4, for a given choice of the parameter values, in the case with Arrhenius relaxation T_e and $T_{e1}^{(\text{is})}$ are very similar. Their difference is one order of magnitude less than in the model with contrived dynamics.

d. A more fundamental definition of the IS effective temperature

Here we propose an alternative way to identify an effective temperature that maps the dynamics between inherent structures into a thermodynamic quantity. We follow a quasi static approach using a partition sum, just as we did in the finite T case. The aim is to be able to define an effective thermodynamic parameter for the IS dynamics and to compare it with the T_e given in (2.41). Following exactly the same approach we used in [3] (see section 2.4), including the substitution of the real external field H with the effective one $H_{e2}^{(\text{is})}$, we compute the partition function counting all the macroscopically equivalent IS's, through which the system is evolving in this symbolic dynamics, at a given time t .

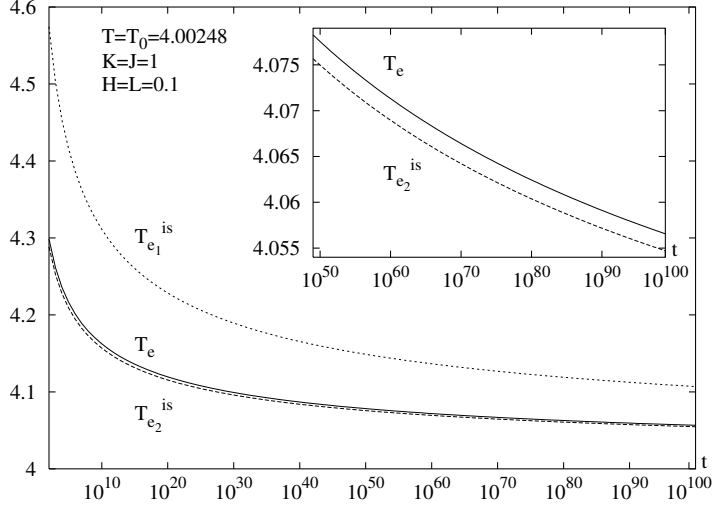


FIG. 3.1. Effective temperatures vs. t at the heat bath temperature $T = 4.00248$, equal to the Kauzmann temperature. The constants in the Hamiltonian (2.1) are set to the following values: $K = J = 1$, $H = L = 0.1$. The constraint constant is $m_0 = 5$. The upper curve shows the effective temperature got by matching out of equilibrium and equilibrium IS internal energy. The one in the middle is the behavior of (2.41), for systems at finite T , and the lowest one is the IS effective temperature (3.29).

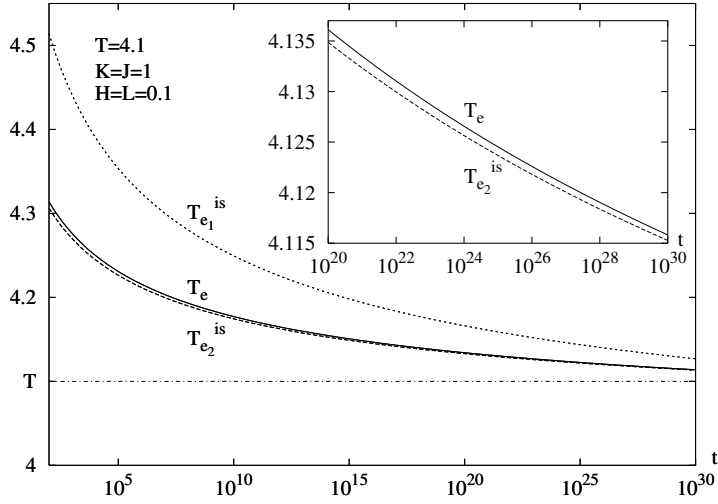


FIG. 3.2. The same effective temperatures, for the same choice of parameters as before are plotted for a different heat bath temperature: $T = 4.1$.

$$Z_e^{(\text{is})}(m_1, m_2) = \int \mathcal{D}x \exp \left[-\beta_{e2}^{(\text{is})} \mathcal{H}_{\text{is}} \left(\{x_i\}; T, H_{e2}^{(\text{is})} \right) \right] \delta \left(Nm_1 - \sum_i x_i \right) \delta \left(Nm_2 - \sum_i x_i^2 \right) = \quad (3.24)$$

$$= \exp \left\{ -\beta_{e2}^{(\text{is})} N \left[\frac{K}{2} m_2 - H_{e2}^{(\text{is})} m_1 - \bar{w}_{\text{is}} - \frac{T_{e2}^{(\text{is})}}{2} \log (m_2 - m_1^2) \right] \right\} = \quad (3.25)$$

$$\simeq \exp \left\{ -\beta_{e2}^{(\text{is})} \left[\mathcal{H}_{\text{is}} \left(m_1, m_2; T, H_{e2}^{(\text{is})} \right) - T_{e2}^{(\text{is})} \mathcal{I} \left(m_1, m_2 \right) \right] \right\}. \quad (3.26)$$

$\beta_{e2}^{(\text{is})} = 1/T_{e2}^{(\text{is})}$ and $H_{e2}^{(\text{is})}$ are parameters describing the behavior of the system going only through IS's. Minimizing the free energy $F_e^{(\text{is})} \equiv -T_{e2}^{(\text{is})} \log Z_e^{(\text{is})}$ with respect to $m_{1,2}$ we get:

$$T_{e2}^{(\text{is})} = \tilde{K}_{\text{is}}(m_1, m_2) [m_2 - m_1^2], \quad (3.27)$$

$$H_{e2}^{(\text{is})} = H - \tilde{K}_{\text{is}}(m_1, m_2) \mu_1. \quad (3.28)$$

By inserting the time dependent values of m_1 and m_2 we now look at the time evolution of the effective temperature (3.27) for large times, in the aging regime, and we compare it with the behavior of the thermodynamic effective temperature (2.41).

For the dynamically constrained model, for $t \rightarrow \infty$, $T_{e2}^{(is)} \rightarrow T$ (if $T > T_0$). When $t_0 \ll t < \infty$, however, the way the effective temperature approach the heat bath temperature is different from the behavior (2.41) of T_e , found in the case at finite temperature. For a comparison their first order expansions are:

$$T_{e2}^{(is)} \simeq T + \left(1 + T \frac{\tilde{K}_{is,\infty}(T) Q_\infty^{(is)} J^2}{2D(1 + Q_\infty^{(is)} D)} \right) \tilde{K}_{is,\infty}(T) \delta\mu_2(t) \quad (3.29)$$

$$T_e \simeq T + \left(1 + T \frac{\tilde{K}_\infty(T) Q_\infty J^2}{2D(1 + Q_\infty D)} \right) \tilde{K}_\infty(T) \delta\mu_2(t) \quad (3.30)$$

where

$$\tilde{K}_{is,\infty}(T) = \lim_{t \rightarrow \infty} \tilde{K}_{is}(m_1(t), m_2(t); T) , \quad (3.31)$$

$$\tilde{K}_\infty(T) = \lim_{t \rightarrow \infty} \tilde{K}(m_1(t), m_2(t); T) ,$$

$$Q_\infty^{(is)} = \lim_{t \rightarrow \infty} \frac{J^2 D}{\tilde{K}_{is}^3 w_{is}^3} , \quad (3.32)$$

$$Q_\infty = \lim_{t \rightarrow \infty} Q = \lim_{t \rightarrow \infty} \frac{J^2 D}{\tilde{K}^3 w (w + T/2)^2} . \quad (3.33)$$

The time dependent variable $\delta\mu_2(t)$ is introduced in (2.33) in both cases (apart from the parameter t_0 influencing only the short times) while the coefficients in front of it are different at any temperature, including T_0 . In the fragile case, thus, this second IS effective temperature does not coincide with $T_{e1}^{(is)}$ and it is much nearer, at any time, to (3.30). However, even if this $T_{e2}^{(is)}$ is conceptually more properly chosen than the one defined matching out of equilibrium energy at temperature T and equilibrium energy at temperature $T_e^{(is)}$, we still do not get the same parameter describing the finite T dynamics in a thermodynamic frame. The inherent structure approach gives thus a good approximation but is nevertheless never analytically correct.

To show how good this approximation is we can take as an instance a certain realization of the model with given values of the “fields” and “coupling constants”. We plot in figures 3.1 and 3.2 the behavior of $T_{e1}^{(is)}(t)$, $T_{e2}^{(is)}(t)$ and $T_e(t)$ at heat-bath temperatures equal to and just above the Kauzmann temperature.

For the strong glass case we also expand for temperatures near to zero and for long time and we get:

$$T_{e2}^{(is)}(t) = T + \tilde{K}_{is} \delta\mu_2(t) = T + \frac{KD}{D + J^2} \delta\mu_2(t) + \frac{T}{2} \frac{J^4 K^2}{(D + J^2)^3} \delta\mu_2(t) + \frac{DJ^4 K^3}{2(D + J^2)^4} \delta\mu_2(t)^2 \quad (3.34)$$

$$+ \mathcal{O}(T^3) + \mathcal{O}(T^2 \delta\mu_2(t)) + \mathcal{O}(T \delta\mu_2(t)^2) + \mathcal{O}(\delta\mu_2(t)^3)$$

$$= T_e(t) - \frac{DJ^2 K^2}{2(D + J^2)^3} T \delta\mu_2(t) + \mathcal{O}(\delta\mu_2(t)^3) + \mathcal{O}(T^3) + \mathcal{O}(T^2 \delta\mu_2(t)) + \mathcal{O}(T \delta\mu_2(t)^2) \quad (3.35)$$

$$= T_{e1}^{(is)}(t) + \frac{DJ^4 K^3}{2(D + J^2)^4} \delta\mu_2(t)^2 + \mathcal{O}(T^3) + \mathcal{O}(T^2 \delta\mu_2(t)) + \mathcal{O}(T \delta\mu_2(t)^2) + \mathcal{O}(\delta\mu_2(t)^3) \quad (3.36)$$

where $\delta\mu_2$ is given by (2.37).

The effective temperature T_e mapping the dynamics of the system evolving at finite temperature T have the same behavior of T_{e2} in approaching the heat-bath temperature up to order $T \delta\mu_2(t)$ where they start deviating one from the other. For a quenching to zero temperature the two effective temperatures coincide. Moreover, due to the simplicity of the model, the IS effective temperature $T_{e2}^{(is)}$ is equal to with $T_{e1}^{(is)}$ given in (3.21) up to order $\delta\mu_2(t)$ in time and up to order T^3 in temperature.

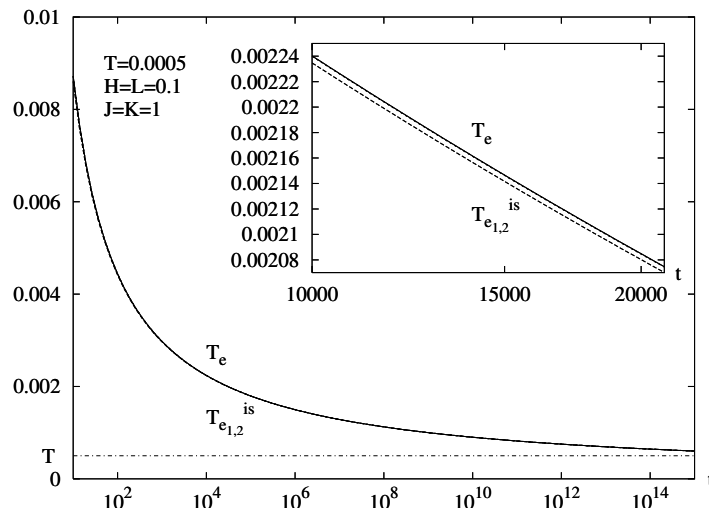


FIG. 3.3. Time evolution of the effective temperatures at the heat bath temperature $T = 0.0005$ in the model with Arrhenius relaxation. The constants in the Hamiltonian (2.1) are set to the following values: $K = J = 1$, $H = L = 0.1$. The lower curve shows the effective temperature (3.21) got by matching out of equilibrium and equilibrium IS internal energy. To order $\delta\mu_2$ it coincides analytically with the IS effective temperature (3.35). Second order differences are too small to appear in the plot. The upper curve is the behavior of (2.41), for systems at finite T .

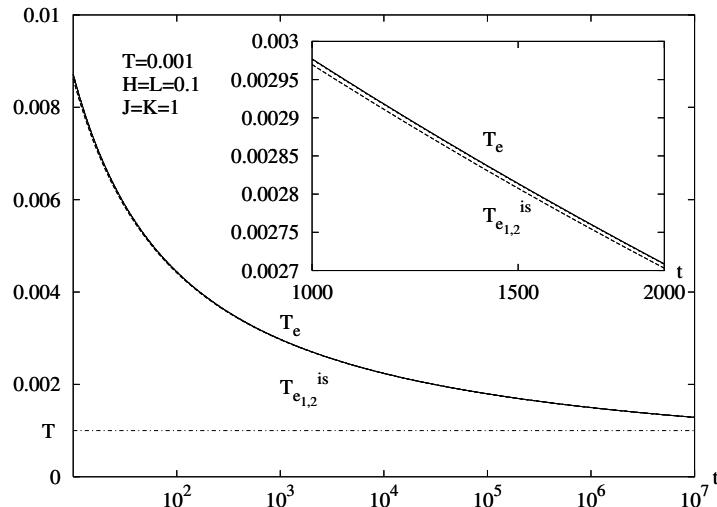


FIG. 3.4. The same effective temperatures, for the same choice of parameters as before are plotted for a different heat bath temperature: $T = 0.001$. Comparing the time scales of the two plots, we can clearly observe the decreasing of the Arrhenius relaxation time to equilibrium τ_{eq} that takes place rising the temperature.

4. CONCLUSIONS

In this paper we consider a model that owns all the basic properties of a glass, built by processes evolving on two well separated time scales, representing the α and β processes taking place in real glassy materials [3]. The decoupling of time scales is fundamental for a generalization of equilibrium thermodynamics to systems far from equilibrium.

We take into account two different versions of the model given by (2.1). One leading to the description of a fragile glass having a non-zero Kauzmann temperature and the other one representing a strong glass.

Using a particular Monte Carlo dynamics and developing it analytically, thus having the opportunity of probing it in more detail with respect to a numeric study, we found equations of motion that are in all respect those typical of glass relaxation.

In the strong glass case we apply exactly the same parallel Monte Carlo dynamics used in [14–16,23], finding an

Arrhenius relation between the relaxation time of the slow processes $\{x_i\}$ and the temperature.

In the fragile glass case the model is provided with a constraint applied to the harmonic oscillator dynamics, i. e. to the slow processes dynamics, in order to reproduce the behavior of a good fragile glass former. In [3], by means of a Monte Carlo constrained dynamics, we identified the Kauzmann temperature with the one, T_0 , at which the constraint is reached, asymptotically, for the first time in a cooling experiment from high temperature. There we showed how the thermodynamic phase transition [25] is characterized, that takes place due to the breaking of the ergodicity in the landscape of our model, rich of degenerate minima.

In this work we carried out the inherent structure approach. In both dynamical models, decreasing the temperature, the free energy local minima do not split into smaller local minima, just like in the p -spin model in zero magnetic field [26], because every allowed configuration of harmonic oscillators is and stays an inherent structure at any temperature. Consequently we can set a one-to-one correspondence between the minima of the free energy and the ones of the potential energy (i. e. the inherent structures). Because of this exact correspondence the dynamics through inherent structures should be a valid symbolic dynamics for the real system, i.e. at a finite heat-bath temperature T . At least, it would significantly represents the actual dynamics if the inherent structures are visited with the same frequency with which the corresponding free energy minima at finite T are visited.

We defined the steepest descent procedure for the model, that is the minimization of the effective Hamiltonian (2.5) appearing in the partition function with respect to the spins, i. e. the fast relaxing variables. Due to the minimization any explicit dependence on T disappears. The configurational entropy for inherent structures was computed from the logarithm of the Jacobian of the transformation of variables $\mathcal{D}x \rightarrow dm_1 dm_2$, and thus it was the same of the exact finite T approach. In our models, then, any configuration of harmonic oscillators $\{x_i\}$ (for the fragile glass model every configuration allowed by the constraint), is also an inherent structure. Although the models we considered are conceptually very simple and without interactions, as compared to another approach proposed for systems with interacting discrete spins where the IS scheme breaks down [27], our setup seems to be more physical since it is intimately based on time scale separation between fast and slow processes. A direct consequence of this time scale separation is that we encounter a both mathematically and physically well defined configurational entropy, whereas this observable suffers from principle difficulties in [27].

We can take a system in equilibrium at an effective temperature $T_e^{(is)}$, such that the configurations visited by the system at equilibrium are the same as those out of equilibrium at temperature T . First we defined an effective temperature through the matching of the equilibrium and the out of equilibrium internal energy of the inherent structures (the one such that $E(T_e(t)) = E_d(t)$). For the strong glass model this effective temperature almost coincides with the finite temperature T_e provided that the temperature at which the system is quenched is not too high (as far as terms of $\mathcal{O}(T\delta\mu_2(t))$ are negligible they are equal). On the contrary, when the constraint is set and the contrived Monte Carlo dynamics is applied, we found that the thus derived effective temperature $T_{e1}^{(is)}$ is quite different from the effective temperature that we were able to identify in the finite T dynamics. Therefore we proposed a new definition following a quasi static approach. In this way we computed the partition function counting all the macroscopically equivalent inherent structures, through which the system is evolving in this symbolic dynamics, at a given time t . Even though the result we get is much more similar to the finite T dynamics effective temperature (numerically speaking the difference is one order of magnitude smaller), yet it is analytically different, indicating that the inherent structure scheme can only be an approximation to what happens in the realistic dynamics of the system. As a consequence, also the derivation of out of equilibrium thermodynamic quantities (e.g. the configurational entropy) obtained making use of this approach could suffer of a systematic deviation from the exact result.

ACKNOWLEDGMENTS

We thank F. Ritort for suggestions and a careful reading of the manuscript. We also thank A. Crisanti and F. Sciortino for useful discussions. The research of L. Leuzzi is supported by FOM (The Netherlands).

APPENDIX: STRONG GLASS DYNAMICS

In this appendix we present the Monte Carlo dynamics of the observables μ_1 and μ_2 , functions of the slow relaxing harmonic oscillators $\{x_i\}$ through

$$m_1 = \frac{1}{N} \sum_i x_i, \quad , \quad m_2 = \frac{1}{N} \sum_i x_i^2, \quad (\text{A.1})$$

in the case where the model (2.1) is not subjected to any constraint on its $\{x_i\}$ configurations.

Let us recall the definitions, given in section 2.3,

$$\mu_1 \equiv \frac{\tilde{H}}{\tilde{K}} - m_1 \quad (\text{A.2})$$

$$\mu_2 \equiv m_2 - m_1^2 \quad (\text{A.3})$$

In this notation the average and the variance (2.23) of the gaussian distribution $p(x|m_1, m_2)$ (see (2.21)) of the possible changes in energy during the Monte Carlo dynamics become:

$$\bar{x} = \frac{\Delta^2 \tilde{K}}{2} \quad , \quad \Delta_x = \Delta^2 \tilde{K}^2 (\mu_2 + \mu_1^2) \quad . \quad (\text{A.4})$$

We remember here that x is the difference (2.20) between the energy of the configuration proposed for the exchange and the energy of the actual configuration. Δ is fixed.

To shorten the following expressions we also define the parameter

$$\alpha \equiv \frac{\bar{x}}{\sqrt{2\Delta_x}} = \sqrt{\frac{\Delta^2}{8(\mu_2 + \mu_1^2)}} \quad (\text{A.5})$$

The two basic quantities that have to be computed in order to solve the dynamic equations for μ_1 and μ_2 are the acceptance rate of the Monte Carlo updating:

$$A(t) \equiv \int dx W(\beta x) p(x|m_1, m_2) \quad (\text{A.6})$$

and the rate of change of the energy of the system:

$$I_1(t) \equiv \int dx x W(\beta x) p(x|m_1, m_2) \quad (\text{A.7})$$

Defining the auxiliary function:

$$f(t) \equiv \bar{x}\beta \exp\left(-\beta\bar{x} + \frac{\beta^2\Delta_x}{2}\right) \text{erfc}\left(\sqrt{\frac{\Delta_x}{\bar{x}}}\beta - \alpha\right) \quad , \quad (\text{A.8})$$

where

$$\text{erfc}(a) \equiv \frac{2}{\sqrt{\pi}} \int_a^\infty dz e^{-z^2} \quad , \quad (\text{A.9})$$

we can write down the exact expressions for A and I_1 as

$$A = \frac{1}{2} \left[\text{erfc}(\alpha) + \frac{f}{\beta\bar{x}} \right] \quad (\text{A.10})$$

$$I_1 = \frac{\bar{x}}{2} \left[\text{erfc}(\alpha) + \left(1 - \frac{\beta\bar{x}}{2\alpha^2}\right) \frac{f}{\beta\bar{x}} \right] \quad (\text{A.11})$$

The Monte Carlo equations of motion for μ_1 and μ_2 are formally the same found for the fragile glass case [3]:

$$\dot{\mu}_1 = -JQ \int dx x W(\beta x) p(x|m_1, m_2) - (1 + DQ) \int dx \bar{y}(x) W(\beta x) p(x|m_1, m_2) \quad (\text{A.12})$$

$$\dot{\mu}_2 = \frac{2}{\tilde{K}} \int dx x W(\beta x) p(x|m_1, m_2) + 2\mu_1 \int dx \bar{y}(x) W(\beta x) p(x|m_1, m_2) \quad (\text{A.13})$$

From (2.23) we know $\bar{y}(x)$ and we can rewrite it as a function of the above defined α :

$$\bar{y}(x) = 4\alpha^2\mu_1 \left(1 - \frac{x}{\bar{x}}\right) \quad (\text{A.14})$$

Using this we get

$$\dot{\mu}_1 = - \left(JQ - \frac{8\alpha^2\mu_1(1 + DQ)}{\Delta^2\tilde{K}} \right) I_1(t) - 4\alpha^2\mu_1(1 + DQ)A(t) \quad (\text{A.15})$$

$$\dot{\mu}_2 = \frac{2}{\tilde{K}} \left(1 - \frac{8\alpha^2\mu_1^2}{\Delta^2\tilde{K}} \right) I_1(t) + 8\alpha^2\mu_1^2 A(t) \quad (\text{A.16})$$

1. Dynamics in the aging regime: zero temperature

First of all we solve the equation of motion for μ_2 at $T = 0$, neglecting terms of order μ_1^2 with respect to those of order μ_2 . For long times is $\alpha \gg 1$. We can, then, expand $I_1(t)$ for large α , getting

$$I_1(t) \simeq -\frac{e^{-\alpha^2}}{2\alpha\sqrt{\pi}} \frac{\Delta^2 \tilde{K}}{4\alpha^2} \quad (\text{A.17})$$

Equation (A.16) becomes then

$$\dot{\mu}_2 \simeq -\frac{e^{-\alpha^2}}{2\alpha\sqrt{\pi}} \frac{\Delta^2}{4\alpha^2}, \quad (\text{A.18})$$

otherwise written as

$$\dot{\alpha} \simeq \frac{e^{-\alpha^2}}{\sqrt{\pi}} \quad (\text{A.19})$$

or

$$\dot{\mu}_2 \simeq -2\mu_2^{3/2} \frac{\exp\left(-\frac{\Delta^2}{8\mu_2}\right)}{\sqrt{\pi}} \quad (\text{A.20})$$

At $T = 0$, the solution in the aging regime, expressed in $\mu_2 \simeq \Delta^2/(8\alpha^2)$, turns out to be:

$$\mu_2(t) \simeq \frac{\Delta^2}{8} \frac{1}{\log \frac{2t}{\sqrt{\pi}} + \frac{1}{2} \log \log \frac{2t}{\sqrt{\pi}}}. \quad (\text{A.21})$$

Always at zero temperature the leading order of the expansion of the acceptance rate A is , for $\alpha \gg 1$,

$$A \simeq \frac{e^{-\alpha^2}}{2\alpha\sqrt{\pi}} \quad (\text{A.22})$$

Combining this with (A.17), the Monte Carlo equation of motion (A.15) takes the form

$$\dot{\mu}_1 = \frac{e^{-\alpha^2}}{2\alpha\sqrt{\pi}} \left\{ \frac{JQ\Delta^2\tilde{K}}{4\alpha^2} - 2\mu_1(1 + DQ)(2\alpha^2 + 1) \right\} \quad (\text{A.23})$$

Dividing (A.23) for (A.18) we can write down a differential equation for μ_1 as a function of μ_2 :

$$\frac{d\mu_1}{d\mu_2} \simeq 16(1 + DQ) \frac{\alpha^4}{\Delta^2} \mu_1 - JQ\tilde{K} \quad (\text{A.24})$$

where we have neglected terms of order $1/\alpha^2$ with respect to those of order 1. In the adiabatic approximation, obtained by neglecting the left hand side, the solution of (A.24) turns out to be

$$\mu_1 \simeq \frac{4JQ\tilde{K}}{\Delta^2(1 + DQ)} \mu_2^2 \quad (\text{A.25})$$

At zero temperature and for long times, one thus have $\mu_1 \sim \mu_2^2 \ll \mu_2$.

2. Dynamics in the aging regime: $T > 0$

If T is above zero, the leading order of the expansion of A and I_1 for large times ($\alpha \gg 1$) and small temperature are:

$$A \simeq \frac{e^{-\alpha^2}}{2\alpha\sqrt{\pi}} \frac{1}{1 - \frac{4T\alpha^2}{\Delta^2\tilde{K}}} \quad (\text{A.26})$$

$$I_1 \simeq \frac{e^{-\alpha^2}}{2\alpha\sqrt{\pi}} \frac{\Delta^2\tilde{K}}{4\alpha^2} \frac{1 - \frac{8T\alpha^2}{\Delta^2\tilde{K}}}{\left(1 - \frac{4T\alpha^2}{\Delta^2\tilde{K}}\right)} \quad (\text{A.27})$$

where the terms $T\alpha^2$ are of $\mathcal{O}(1)$. Indeed it is

$$\frac{8T\alpha^2}{\Delta^2\tilde{K}} = \frac{8T}{\Delta^2\tilde{K}} \frac{\Delta^2}{8\mu_2} = \frac{\bar{\mu}_2}{\mu_2} = \frac{1}{1 + \frac{\delta\mu_2}{\mu_2}}, \quad (\text{A.28})$$

(see the definition of α (A.5)) so that

$$\lim_{t \rightarrow \infty} \frac{8T\alpha^2}{\Delta^2\tilde{K}} = 1, \quad T > 0. \quad (\text{A.29})$$

In this notation (A.26) and (A.27) can be rewritten also as

$$A = \frac{e^{-\alpha^2}}{\alpha\sqrt{\pi}} \frac{1 + \frac{\delta\mu_2}{\mu_2}}{1 + 2\frac{\delta\mu_2}{\mu_2}} \quad (\text{A.30})$$

$$I_1 = -\frac{e^{-\alpha^2}}{\alpha\sqrt{\pi}} \frac{\Delta^2\tilde{K}}{\alpha^2} \frac{\delta\mu_2}{\bar{\mu}_2} \frac{1 + \frac{\delta\mu_2}{\mu_2}}{\left(1 + 2\frac{\delta\mu_2}{\mu_2}\right)^2} \quad (\text{A.31})$$

and the Monte Carlo equations are now

$$\dot{\mu}_1 \simeq \frac{e^{-\alpha^2}}{\alpha\sqrt{\pi}} \frac{1 + \frac{\delta\mu_2}{\mu_2}}{1 + 2\frac{\delta\mu_2}{\mu_2}} \left[-4\alpha^2(1 + DQ)\mu_1 + \frac{JQ\Delta^2\tilde{K}}{2\alpha^2} \frac{\delta\mu_2}{\bar{\mu}_2} \frac{1}{1 + 2\frac{\delta\mu_2}{\mu_2}} \right] \quad (\text{A.32})$$

$$\dot{\mu}_2 \simeq \frac{e^{-\alpha^2}}{\alpha\sqrt{\pi}} \frac{\Delta^2}{\alpha^2} \frac{\delta\mu_2}{\bar{\mu}_2} \frac{1 + \frac{\delta\mu_2}{\mu_2}}{\left(1 + 2\frac{\delta\mu_2}{\mu_2}\right)^2} \quad (\text{A.33})$$

The solution to (A.33) is, to leading order,

$$\mu_2(t) \simeq \frac{\Delta^2}{8} \frac{1}{\log \frac{2t}{\sqrt{\pi}}}. \quad (\text{A.34})$$

The behaviour of μ_1 comes out to be

$$\mu_1 \simeq \frac{4JQ\tilde{K}}{\Delta^2(1 + DQ)} \mu_2^2 \frac{\delta\mu_2}{\bar{\mu}_2} \frac{2}{1 + 2\frac{\delta\mu_2}{\mu_2}}. \quad (\text{A.35})$$

Notice that this vanishes when equilibrium is approached, since then $\delta\mu_2 \rightarrow 0$.

For times even longer than the time scale of the aging regime, the system finally relax, exponentially fast, to equilibrium. The equilibrium value of μ_2 is known from the statics (see section 2), as

$$\bar{\mu}_2 = \frac{T}{\tilde{K}_\infty(T)} \quad (\text{A.36})$$

where the explicit expansion of $\tilde{K}_\infty(T)$ in temperature is shown in (2.38). The asymptotic value of α is, from its definition (A.5) and taking the first order expansion in T ,

$$\alpha(T) = \sqrt{\frac{\Delta^2}{8\bar{\mu}_2(T)}} \simeq \sqrt{\frac{A_s}{T}} \quad (\text{A.37})$$

with

$$A_s \equiv \frac{\Delta^2 K D}{8(D + J^2)} . \quad (\text{A.38})$$

From the equations of motion studied above (look for instance at (A.19)) we find for the relaxation time to equilibrium

$$\tau_{\text{eq}} \propto e^{\alpha^2} . \quad (\text{A.39})$$

Using (A.37) this is nothing else than the Arrhenius law

$$\tau_{\text{eq}} \sim \exp\left(\frac{A_s}{T}\right) . \quad (\text{A.40})$$

-
- [1] C.A. Angell, *Science* **267** (1995) 1924.
 - [2] G.B. McKenna, in *Comprehensive Polymer Science 2: Polymer Properties*, C. Booth and C. Price, eds. (Pergamon, Oxford, 1989), pp 311.
 - [3] L. Leuzzi, T.M. Nieuwenhuizen, cond-mat/0101304.
 - [4] F.H. Stillinger, T.A. Weber, *Phys. Rev. A* **25** (1982) 978.
 - [5] F.H. Stillinger, T.A. Weber, *Science* **225** (1984).
 - [6] F.H. Stillinger, T.A. Weber, *Science* **267** (1995) 1935.
 - [7] S. Sastry, P.G. De Benedetti, *Nature* **393** (1998) 554.
 - [8] W. Kob, F. Sciortino, P. Tartaglia, *Europhys. Lett.* **49** (1999) 590.
 - [9] F. Sciortino, W. Kob, P. Tartaglia, *Phys. Rev. Lett.* **83** (1999) 3214.
 - [10] A. Crisanti, F. Ritort, *Physica A* **280** (2000) 155.
 - [11] A. Crisanti, F. Ritort, *Europhys. Lett.* **51** (2000) 147.
 - [12] A. Crisanti, F. Ritort, *Europhys. Lett.* **52** (2000) 640.
 - [13] Th.M. Nieuwenhuizen, cond-mat/9911052.
 - [14] L.L. Bonilla, F.G. Padilla, G. Parisi, F. Ritort, *Phys. Rev. B* **54** (1996) 4170.
 - [15] L.L. Bonilla, F.G. Padilla, and F. Ritort, *Physica A* **250** (1998) 315
 - [16] Th.M. Nieuwenhuizen, *Phys. Rev. Lett.* **80** (1998) 5580.
 - [17] R. J. Glauber, *J. Math. Phys.*, **4** (1963) 294.
 - [18] G. H. Fredrickson, H.C. Andersen, *Phys. Rev. Lett.* **53** (1984) 1244.
 - [19] E. Follana, F. Ritort, *Phys. Rev. B*, **54** (1996) 930.
 - [20] W. Kob, H.C. Andersen, *Phys. Rev. E* **48** (1993) 4364.
 - [21] J. Kurchan, L. Peliti, M. Sellitto, *Europhys. Lett.* **39** (1997) 365.
 - [22] H. Vogel, *Physik. Z.* **22** (1921) 645;
G.S. Fulcher, *J. Am. Ceram. Soc.* **8** (1925) 339;
G. Tammann and G. Hesse, *Z. Anorg. Allgem. Chem.* **156** (1926) 245.
 - [23] Th.M. Nieuwenhuizen, *Phys. Rev. E*, **61** (2000) 267.
 - [24] A. Garriga, F. Ritort, cond-mat/0009428.
 - [25] W. Kauzmann, *Chem. Rev.* **43** (1948) 219.
 - [26] A. Crisanti, H.J. Sommers, *J. Phys.* **5** (1995) 805.
 - [27] G. Biroli, R. Monasson, *Europhys. Lett.* **50** (2000) 155.